

Selected papers presented at the 15th Symposium of Magnetic Measurements and Modelling SMMM'2025

Modeling of Magnetocaloric Effect in Amorphous Fe-Based Ribbons

I. BIALIK AND P. GEBARA*

Department of Physics, Czestochowa University of Technology, Armii Krajowej 19, 42-200 Czestochowa, Poland

Doi: [10.12693/APhysPolA.149.S109](https://doi.org/10.12693/APhysPolA.149.S109)

*e-mail: piotr.gebara@pcz.pl

In this paper, phenomenological modeling and experimental studies were conducted to predict magnetocaloric properties of the $\text{Fe}_{76}\text{Mo}_{10}\text{Cu}_1\text{B}_{13}$ alloy. The temperature dependence of magnetization was measured and calculated. A good correlation between simulated and experimentally determined data was observed. The phenomenological model allowed us to obtain theoretical values of the magnetic entropy change, the full width at half maximum of the ΔS_M vs T curve, and the relative cooling power.

topics: magnetocaloric materials, magnetic entropy change, relative cooling power

1. Introduction

For almost thirty years, scientists all over the world have been conducting research aimed at protecting the natural environment and saving energy. The elimination of freon compounds is the most important way to save Earth's atmosphere. These compounds act as active regenerators in cooling devices, i.e., domestic refrigerators. Such devices operate on the basis of compression/decompression processes of freon gas, with efficiency reaching even 45%. A more efficient technique of lowering temperature is based on the magnetocaloric effect [1]. This phenomenon is observed as temperature variation of a magnetic material under changes in the external magnetic field. Since the discovery of the giant magnetocaloric effect in the $\text{Gd}_5\text{Ge}_2\text{Si}_2$ alloy by Pecharsky and Gschneider [2], many different materials have been developed in order to improve their thermomagnetic properties. These are, for example, pure Gd and its alloys [2–5], the $\text{La}(\text{Fe}, \text{Si})_{13}$ -type alloys [6–8], MM'X [10–15] alloys, or Heusler alloys [16].

Another interesting group is Fe-based amorphous or nanocrystalline alloys [17–19]. Taking into account the excellent magnetic properties of the Fe-based amorphous or nanocrystalline alloys, they are good candidates for active elements in magnetic refrigerators. Nowadays, research on novel magnetocaloric alloys could be supported by simulation techniques. An interesting model that allows

the prediction of magnetocaloric properties was proposed by Hamad in [20]. It was successfully applied to MnCoGe [21, 22] and $\text{LaFe}_{11.0}\text{Co}_{0.8}\text{Si}_{1.2}$ alloys [23].

The aim of the present work is to verify the usefulness of the Hamad model applied to experimental data on the $\text{Fe}_{76}\text{Mo}_{10}\text{Cu}_1\text{B}_{13}$ alloy.

2. Experimental techniques

An ingot sample of the $\text{Fe}_{76}\text{Mo}_{10}\text{Cu}_1\text{B}_{13}$ alloy was obtained by arc-melting of high-purity constituent elements under a low pressure of Ar. The sample was remelted ten times in order to ensure its homogeneity. Ribbons were produced by the melt-spinning method in an Ar protective atmosphere. X-ray diffraction was carried out using a Bruker D8 ADVANCE diffractometer with $\text{Cu } K_\alpha$ radiation and LynxEye detector. Magnetic properties were studied using VersaLab Quantum Design (vibrating sample magnetometer, i.e., VSM option) in a magnetic field of up to 2 T and over a wide range of temperatures. The magnetic entropy change was calculated using the Maxwell equation [4]

$$\Delta S_M(T, \Delta H) = \mu_0 \int_0^H dH \left(\frac{\partial M(T, H)}{\partial T} \right)_H, \quad (1)$$

where μ_0 is the magnetic permeability of vacuum, H is the strength of the magnetic field, M is the magnetization, and T is the temperature.

The relative cooling power (*RCP*) parameter was calculated based on the following relation [16]

$$RCP = -\Delta S_{M \max} \delta T_{FWHM}, \quad (2)$$

where δT_{FWHM} means the full width at half maximum (FWHM) of the magnetic entropy change peak ΔS_M .

3. Phenomenological model

In order to predict magnetization variations upon temperature, Hamad proposed a phenomenological model in [20], taking into account the following equation

$$M = \frac{M_i + M_f}{2} \tanh(A(T_C - T)) + BT + C, \quad (3)$$

where T_C , M_i , and M_f denote the following physical magnitudes: the Curie temperature, an initial magnetization, and final magnetization at ferromagnetic–paramagnetic transition, respectively. The necessary values of parameters A , B , and C needed to conduct modeling were obtained from the experimental temperature dependence of magnetization (M vs T curve, which is presented in Fig. 1). Selected points were marked in Fig. 1 and were used for calculations of the A , B , and C parameters described by following formulas

$$A = \frac{2(B - S_C)}{M_i - M_f}, \quad (4)$$

$$B = \frac{dM}{dT}, \quad (5)$$

$$C = \frac{M_i - M_f}{2} - BT_C, \quad (6)$$

$$S_C = \frac{dM}{dT} \quad \text{at} \quad T = T_C. \quad (7)$$

Taking into account relations (1) and (3)–(7), the theoretical equation describing temperature evolution of magnetic entropy upon temperature can be rewritten in the following form

$$\Delta S_M = \left[-A \frac{(M_i - M_f)}{2} \operatorname{sech}^2(A(T_C - T)) + B \right] H_{\max}. \quad (8)$$

The value of magnetic entropy change is strongly related to the first derivative of the M vs T curve at the Curie temperature $dM/dT(T_C)$. A value of magnetic entropy change is strongly related to the high magnetic moment and the value of $dM/dT(T_C)$. A relation describing the maximum value of magnetic entropy change can be given in the following form

$$\Delta S_M = \left[-A \frac{(M_i - M_f)}{2} + B \right] H_{\max}. \quad (9)$$

Taking into account the magnetic cooling process, determining the magnetic entropy change and its maximum value for the studied magnetocaloric

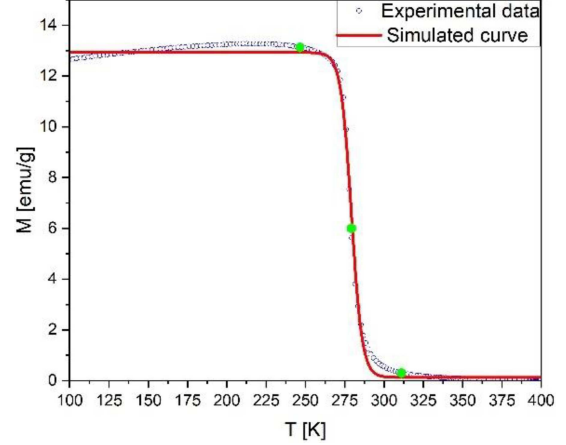


Fig. 1. Experimental and simulated M vs T curves obtained for the $\text{Fe}_{76}\text{Mo}_{10}\text{Cu}_1\text{B}_{13}$ alloy ribbon (under the change in magnetic field ~ 2 T).

TABLE I

Simulated and experimental magnetocaloric properties of the $\text{Fe}_{76}\text{Mo}_{10}\text{Cu}_1\text{B}_{13}$ alloy ribbon under the change in external magnetic field ~ 2 T.

	ΔS_M [J/(kg K)]	δT_{FWHM} [K]	<i>RCP</i> [J/kg]
Exper. value	0.88	120	105
Theor. value	0.79	114	90

material is extremely significant. Another important parameter showing useful properties is the working temperature range of the investigated materials. Commonly, such a parameter is related to the full width at half maximum of the temperature dependence of magnetic entropy change. As it was shown by Hamad [20], this parameter can be calculated using the following relation

$$\delta T_{FWHM} = \frac{2}{A} \cosh^{-1} \left(\sqrt{\frac{2A(M_i - M_f)}{A(M_i - M_f) + 2B}} \right). \quad (10)$$

Based on (10) and applying it to relationships (2) and (9), the relative cooling power can be shown as

$$RCP = \left(M_i - M_f - 2 \frac{B}{A} \right) H_{\max} \times \cosh^{-1} \left(\sqrt{\frac{2A(M_i - M_f)}{A(M_i - M_f) + 2B}} \right). \quad (11)$$

The above formulas (9)–(11) allowed us to predict the most important magnetocaloric parameters. Theoretical and experimental values were compared and turned out to be similar. They are compiled in Table I.

Temperature dependences of magnetization obtained in experiment and theoretical calculations are presented in Fig. 1. The theoretical curve corresponds very well to the measured one. In

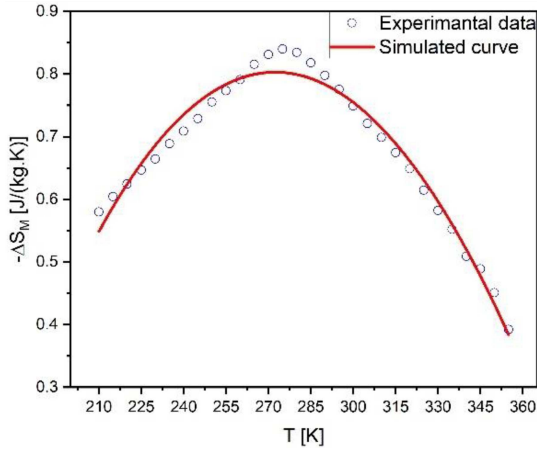


Fig. 2. Experimental and simulated magnetic entropy change for the as-cast $\text{Fe}_{76}\text{Mo}_{10}\text{Cu}_1\text{B}_{13}$ alloy ribbon.

the experimental curve, a characteristic increase in magnetization is observed just before the critical region. It is caused by different temperature dependences of anisotropy and magnetization [17]. The anisotropy constant drops faster than magnetization and this process results in rise of magnetization. However, Hamad's model is so simple that it did not provide the possibility to take into account the anisotropy of the material. The dependence of ΔS_M vs T is shown in Fig. 2. Calculated values are slightly lower than experimental values, although they are comparable over the whole studied range. Hamad's model yielded a bit lower values of δT_{FWHM} , and hence, RCP . The simulated maximum entropy change decreased by 10%, while RCP and δT_{FWHM} increased by 14% and 5%, respectively.

As shown above, the simulated values are reliable and comparable to the experimental results.

4. Conclusions

The temperature dependence of magnetization for the $\text{Fe}_{76}\text{Mo}_{10}\text{Cu}_1\text{B}_{13}$ alloy under the change in external magnetic field ~ 2 T was simulated using Hamad's model. It allowed us to calculate thermomagnetic properties of the $\text{Fe}_{76}\text{Mo}_{10}\text{Cu}_1\text{B}_{13}$ alloy, such as magnetic entropy change, relative cooling power, and full width at half maximum. The experimental measurements of the magnetocaloric effect (MCE) were obtained indirectly using magnetic isotherms. The obtained $\text{Fe}_{76}\text{Mo}_{10}\text{Cu}_1\text{B}_{13}$ alloy ribbon could be applied as an active element in a magnetic refrigerator based on its magnetic entropy change value. Calculated values of magnetic entropy change and relative cooling power are reliable and reasonable. Moreover, experimental and theoretical values are close to each other.

References

- [1] A.M. Tishin, Y.I. Spichkin, *The magnetocaloric effect and its applications*, CRC Press, New York 2003.
- [2] V.K. Pecharsky, K.A. Gschneidner Jr., *J. Magn. Magn. Mater.* **200**, 44 (1999).
- [3] Á. Díaz-García, J.Y. Law, P. Gębara, V. Franco, *JOM* **72**, 2845 (2020).
- [4] P. Gębara, M. Hasiak, J. Kovac, M. Rajnak, *Materials* **15**, 7213 (2022).
- [5] V.K. Pecharsky, K.A. Gschneidner Jr., *Phys. Rev. Lett.* **78**, 4494 (1997).
- [6] P. Gębara, P. Pawlik, B. Michalski, J.J. Wysocki, *Acta Phys. Pol. A* **127**, 576 (2015).
- [7] A. Fujita, Y. Akamatsu, K. Fukamichi, *J. Appl. Phys.* **85**, 4756 (1999).
- [8] X.B. Liu, D.H. Ryan, Z. Altounian, *J. Magn. Magn. Mater.* **270**, 305 (2004).
- [9] P. Gębara, J. Kovac, *J. Magn. Magn. Mater.* **454**, 298 (2018).
- [10] K. Kutynia, P. Gębara, *Materials* **14**, 3129 (2021).
- [11] K. Kutynia, A. Przybył, P. Gębara, *Materials* **16**, 5394 (2023).
- [12] S.K. Pal, C. Frommen, S. Kumar, B.C. Hauback, H. Fjellvag, T.G. Woodcock, K. Nielsch, G. Helgesen, *J. Alloys Compd.* **775**, 22 (2019).
- [13] X. Si, K. Zhou, R. Zhang, X. Ma, Z. Zhang, Y. Liu, *Mater. Res. Express* **5**, 126104 (2018).
- [14] K. Synoradzki, *J. Magn. Magn. Mater.* **482**, 219 (2019).
- [15] P. Gębara, Z. Śniadecki, *J. Alloys Compd.* **796**, 153 (2019).
- [16] A. He, V. Svitlyk, Y. Mozharivskyj, *Inorg. Chem.* **56**, 2827 (2017).
- [17] J. Świerczek, M. Hasiak, *IEEE Trans. Magn.* **40**, 2003504 (2014).
- [18] A. Kupczyk, J. Świerczek, M. Hasiak, K. Prusik, J. Zbroszczyk, P. Gębara, *J. Alloys Compd.* **735**, 253 (2018).
- [19] A. Łukiewska, P. Gębara, *Materials* **15**, 34 (2022).
- [20] M.A. Hamad, *Phase Trans.* **85**, 106 (2012).
- [21] P. Gębara, R. Gozdur, K. Chwastek, *Acta Phys. Pol. A* **146**, 41 (2024).
- [22] K. Kutynia, A. Przybył, I. Bialik, A. Kiljan, P. Gębara, *Acta Phys. Pol. A* **147**, 262 (2025).
- [23] P. Gębara, *Acta Phys. Pol. A* **144**, 360 (2023).